# Observational Evidence for Large-Scale Gas Heating in a Galaxy Protocluster at z = 2.30

CHENZE DONG D, KHEE-GAN LEE D, METIN ATA D, HENJAMIN HOROWITZ D, A AND RIEKO MOMOSE D, 6

Kavli Institute for the Physics and Mathematics of the Universe (WPI), UTIAS,
 The University of Tokyo, Kashiwa, Chiba 277-8583, Japan
 The Oskar Klein Centre, Department of Physics, Stockholm University,
 AlbaNova University Centre, SE 106 91 Stockholm, Sweden
 Lawrence Berkeley National Laboratory, 1 Cyclotron Road, Berkeley, CA 94720, USA
 Department of Astrophysical Sciences, Princeton University, Princeton, NJ 08544, USA
 Observatories of the Carnegie Institution for Science,
 813 Santa Barbara Street, Pasadena, CA 91101, USA
 Department of Astronomy, School of Science,
 The University of Tokyo, 7-3-1 Hongo, Bunkyo-ku, Tokyo, 113-0033, Japan

### Submitted to ApJL

#### ABSTRACT

We report a z=2.30 galaxy protocluster (COSTCO-I) in the COSMOS field, where the Lyman- $\alpha$ forest as seen in the CLAMATO IGM tomography survey does not show significant absorption. This departs from the transmission-density relationship (often dubbed the fluctuating Gunn-Peterson approximation; FGPA) usually expected to hold at this epoch, which would lead one to predict strong Ly $\alpha$  absorption at the overdensity. For comparison, we generate mock Lyman- $\alpha$  forest maps by applying FGPA to constrained simulations of the COSMOS density field, and create mocks that incorporate the effects of finite sightline sampling, pixel noise, and Wiener filtering. Averaged over  $r = 15 h^{-1}$  Mpc around the protocluster, the observed Lyman- $\alpha$  forest is consistently more transparent in the real data than in the mocks, indicating a rejection of the null hypothesis that the gas in COSTCO-I follows FGPA (p = 0.0026, or  $2.79\sigma$  significance). It suggests that the large-scale gas associated with COSTCO-I is being heated above the expectations of FGPA, which might be due to either large-scale AGN jet feedback or early gravitational shock heating. COSTCO-I is the first known large-scale region of the IGM that is observed to be transitioning from the optically-thin photoionized regime at Cosmic Noon, to eventually coalesce into an intra-cluster medium (ICM) by z=0. Future observations of similar structures will shed light on the growth of the ICM and allow constraints on AGN feedback mechanisms.

Keywords: Intergalactic medium (813) — Quasar absorption line spectroscopy (1317) — High-redshift galaxy clusters (2007) — N-body simulations (1083) — Intracluster medium (858)

# 1. INTRODUCTION

After the end of hydrogen reionization by  $z \sim 6$ , the vast majority of hydrogen in the universe is ionized and heated. As photon heating is no longer effective in the optically-thin ionized intergalactic medium (IGM), the

Corresponding author: Chenze Dong chenze.dong@ipmu.jp

competition between photon heating and adiabatic cooling gradually erases the thermal history of reionization (Hui & Haiman 2003; Trac et al. 2008). By the "Cosmic Noon" epoch of  $z \sim 2-4$ , this is expected to result in a universal power-law temperature-density relation for the IGM:

$$T \propto (1 + \delta_m)^{\gamma - 1},\tag{1}$$

where T is the temperature of IGM, and  $\delta_m = \rho/\bar{\rho} - 1$  is the underlying matter overdensity traced by the IGM.

 $\gamma$  is the power-law index of the temperature-density relation, which is expected to be  $\gamma \approx 1.5$  from theoretical expectations (Hui & Gnedin 1997); at  $z \sim 2-3$  this has largely been confirmed by Ly $\alpha$  forest observations (Lee et al. 2015; Hiss et al. 2018; Rorai et al. 2018).

The residual neutral hydrogen in the optically-thin, photoionized IGM is detectable as Lyman-alpha (Ly $\alpha$ ) forest absorption<sup>1</sup>, which is often approximated by an analytical relation between matter overdensity and Ly $\alpha$  optical depth  $\tau$ 

$$\tau \propto \frac{T^{-0.7}}{\Gamma_{\rm uv}} (1 + \delta_m)^2 \propto (1 + \delta_m)^{\beta}, \tag{2}$$

in which  $\Gamma_{\rm uv}$  is the background ultraviolet (UV) photoionization rate, and the power-law index  $\beta$  satisfies  $\beta=2-0.7(\gamma-1)$  after substituting in the temperature-density relationship of Equation 1. While this power-law relation, often known as the fluctuating Gunn-Peterson approximation (FGPA), is not expected to be exact, comparisons with hydrodynamical simulations have found that it remains a useful heuristic (Peirani et al. 2014; Sorini et al. 2016) and is useful over a wide range of applications in the z>2 Ly $\alpha$  forest.

At later times (z < 1.5 or lookback times of < 9.5 Gyrs), FGPA is expected to gradually break down as large-scale shocks from non-linear gravitational collapse lead to collisional heating of the IGM. Simultaneously, feedback from galaxies and supermassive black holes are expected to deposit additional energy into the IGM, leading to a complex multi-phase IGM (Cen & Ostriker 2006) at  $z \sim 0$  that still remains to be fully characterized (e.g., Shull et al. 2012; de Graaff et al. 2019).

Galaxy protoclusters — progenitors of the massive galaxy clusters seen at late times - are an interesting testbed for the evolution of cosmic gas, as they collapse earlier than less dense regions of the Universe, and host significant fractions (> 20%) of cosmic star-formation at high redshifts (Chiang et al. 2017). Early searches for  $z \gtrsim 1$  protoclusters were dominated by searches around 'signposts' such as radio galaxies or luminous quasars leading to unrepresentative and incomplete protocluster samples. Over the past decade, however, 'blind' searches in photometric or spectroscopic data have become more common (see Overzier 2016 for a review). Arguably the most sophisticated technique to-date is the application of density reconstructions and constrained simulations on  $z \gtrsim 2$  galaxy redshift surveys covering representative cosmic volumes in the COSMOS field (Ata

et al. 2021, 2022). This has allowed bespoke gravitational modelling of observed 2.0 < z < 2.5 large-scale structures, hence enabling the discovery and characterization of protoclusters down to lower final masses  $(M(z=0) \approx 4-6 \times 10^{14} \, h^{-1} \, M_{\odot})$  than feasible with most other methods.

While the matter associated with low-redshift cluster halos occupy volumes of  $\sim 1 \mathrm{Mpc^3}$ , at  $z \gtrsim 2$  their Lagrangian extent is of order  $\gtrsim (10 \, \mathrm{cMpc})^3$  (Chiang et al. 2013). This is prior to the regime of fully non-linear collapse and gravitational shock-heating, therefore the Ly $\alpha$  absorption from  $z \gtrsim 2$  protoclusters is still expected to trace the density on  $\sim \mathrm{Mpc}$  scales (Miller et al. 2021). This fact has motivated various searches of z > 2 galaxy protoclusters through their Ly $\alpha$  forest absorption (Stark et al. 2015a; Lee et al. 2016; Cai et al. 2016; Ravoux et al. 2020; Qezlou et al. 2022; Newman et al. 2022).

In this Letter, we use the Ata et al. (2022) protocluster sample (and associated data products) in combination with Ly $\alpha$  forest absorption data in the COSMOS field to show that the infalling gas associated with a z=2.30 galaxy protocluster appears to be heated beyond the expectations of the FGPA, over scales of multiple Mpc. Throughout this paper, we adopt a cosmology of  $H_0=100\,h\,\mathrm{km\,s^{-1}\,Mpc^{-1}}=70\,\mathrm{km\,s^{-1}\,Mpc^{-1}},~\Omega_m=0.315,~\mathrm{and}~\Omega_\Lambda=0.685.$  To avoid confusion, we use  $h^{-1}\,\mathrm{Mpc}$  as the unit of comoving distance, and pMpc when discussing physical scales.

#### 2. DATA

# 2.1. The COSTCO-I Galaxy Protocluster

The possible presence of a protocluster at z=2.30 in the COSMOS field was first noted as a compact overdensity of galaxies by Lee et al. (2016), along with the unusually high Ly $\alpha$  transmission given the overdensity. However, no detailed analysis was carried out.

The protocluster was subsequently confirmed by Ata et al. (2022). In this study, they applied the techniques of density reconstructions and constrained simulations to existing large-scale spectroscopic surveys that have targeted galaxies at the  $z \sim 2-3$  epoch in the COSMOS field (e.g. zCOSMOS, VUDS, MOSFIRE; Lilly et al. 2007, Le Fèvre et al. 2015, Kriek et al. 2015). First, in Ata et al. (2021), the COSMIC-BIRTH hybrid Monte-Carlo density reconstruction algorithm (Kitaura et al. 2021) was applied to estimate the underlying density field and corresponding initial density fluctuations (at z = 100) that would eventually evolve to provide the best match for the 2.0 < z < 2.5 spectroscopic galaxy distribution over the central  $\sim 1 \, \rm deg^2$  of COSMOS. This technique computes the Bayesian posterior probability of the possible initial conditions, thus sampling the uncertainties

<sup>&</sup>lt;sup>1</sup> In this paper, "Ly $\alpha$ " absorption refers implicitly to optically-thin forest absorption; we will not discuss optically-thick absorbers.

inherent in the observational data. A subset of the initial condition realizations were used to seed numerical N-body 'constrained' simulations (dubbed the 'COSTCO' suite, Ata et al. 2022) that were ran to z=0 to track the gravitational evolution of the density field traced by the observed galaxies. They then identified galaxy clusters with  $M>2\times 10^{14}~h^{-1}~M_{\odot}$  in the z=0 simulation snapshot, which were then matched to observed structures at 2.0 < z < 2.5. This study confirmed several previously-known protoclusters in COSMOS such the ZFIRE protocluster at z=2.095 (Nanayakkara et al. 2016) and the 'Hyperion' proto-supercluster at  $z\approx 2.45-2.50$  (Cucciati et al. 2018). In addition to these, a number of new protoclusters were also discovered.

COSTCO J100026.4+020940 (hereafter "COSTCO-I"), located at RA =  $150.110^{\circ} \pm 0.042^{\circ}$ , dec =  $2.161^{\circ} \pm$  $0.040^{\circ}$  and  $z=2.298\pm0.007$ , was one of the strongest detections (at  $8.7\sigma$  significance) among these newlydiscovered protoclusters. The final mass was estimated to be  $M(z=0)=(4.6\pm 2.2)\times 10^{14}\,h^{-1}\,M_{\odot}$ . While Ata et al. (2022) did not further examine COSTCO-I in detail, we searched the spectroscopic redshift catalog compiled by Momose et al. (2022) and identified member galaxies of COSTCO-I. Since the position of COSTCO-I varies among the realizations, we adopted the following approach to obtain a robust choice of core members: First, we usd the position of COSTCO-I reported by Ata et al. (2022) as an initial guess for the protocluster center, and selected galaxies within a  $6 h^{-1}$  Mpc transverse radius and line-of-sight (LOS) velocity window of  $|\Delta v| < 600 \,\mathrm{km \, s^{-1}}$ . Then, we iteratively recalculated the protocluster center as the median position of the member galaxies and repeated the member selection until convergence. With this method, we found 7 galaxies in the vicinity of COSTCO-I. Note that these galaxies are merely the putative collapsed core — the full Lagrangian extent that would eventually collapse into the z=0 cluster occupies a larger extent than this. Of these core galaxies, the most massive galaxy has a stellar mass of  $M_* = 5.6 \times 10^{10} M_{\odot}$ . These galaxies are shown in Figure 1, which is an interactive figure that can be viewed online and also has been uploaded to Zenodo.

After identifying the protocluster core, we estimated the group mass,  $M_V$ , in order to set the upper limit to the extent of the intra-group or intra-cluster medium that could already be present at z=2.30. We used the virial theorem approach outlined by Girardi et al. (1998):

$$M_V = \frac{3\pi}{2} \frac{\sigma_p^2 R_p}{G}; \tag{3}$$

G is the gravitational constant, and  $R_p=0.577\,\mathrm{pMpc}$  and  $\sigma_p=361\,\mathrm{km\,s^{-1}}$  are the projected radius and

LOS velocity dispersion respectively, as defined in Girardi et al. (1998)). This yielded a core virial mass of  $M_V = 8.2 \times 10^{13} \, M_{\odot}$ . This estimate assumed that the protocluster core is already virialized, which would set an upper limit on the amount of hot intra-group gas that might be present — if these galaxies do not form a virialized halo, the amount of extended hot gas would be significantly less. We also cannot discount the possibility of the velocity spread being caused by the galaxies being lined up in a filament along the LOS over several Mpc. However, since the COSMOS-BIRTH density reconstruction technique takes peculiar velocities into account, both possibilities (lack of virialization or a LOS filament) are in principle included in the posterior results. In other words, we are confident that COSTCO-I will collapse into a cluster regardless of whether our estimate of the core properties is accurate.

For this analysis, we also had in hand the z = 2.30matter overdensity field,  $\delta_m = \rho/\bar{\rho} - 1$ , where  $\rho$  is the matter density, from 57 constrained realizations of the COSTCO N-body simulation suite that was designed to match the observed COSMOS galaxy distribution. These simulation outputs have a box size of  $L_{\text{box}} = 512 \, h^{-1} \, \text{Mpc}$  and are binned in  $256^3$  grid cells, covering the COSMOS volume in the redshift range 2.00 < z < 2.52. The second panel of Figure 2 shows the matter density contrast from one realization of COSTCO in the vicinity of the COSTCO-I protocluster. Note that the barycenter of COSTCO-I in this particular COSTCO realization shown in Figure 2 is slightly offset from the reported position by Ata et al. (2022), which comes from averaging over all the realizations in the COSTCO suite. This illustrates the fact that the ensemble of COSTCO realizations represents a posterior sample encapsulating our uncertainties regarding the protocluster masses and positions.

#### 2.2. Ly\alpha Forest Absorption Data

We now briefly describe the Ly $\alpha$  forest absorption maps that we used to study the large-scale gas in the COSTCO-I protocluster, which is from the CLAMATO survey (Lee et al. 2014, 2018; Horowitz et al. 2022).

The CLAMATO survey was a spectroscopic survey that targeted  $z \sim 2-3$  UV-bright background sources that probe the Ly $\alpha$  forest in the COSMOS field, using the LRIS spectrograph on the Keck-I telescope. For the first time, star-forming galaxies were also systematically targeted as background sources in addition to the traditional quasars. This enabled a high density of Ly $\alpha$  forest sightlines on the sky (857 deg<sup>-2</sup>) which yielded a mean transverse separation of 2.35  $h^{-1}$  Mpc over a footprint of  $\sim$ 0.2 deg<sup>2</sup> in the center of the COSMOS field.

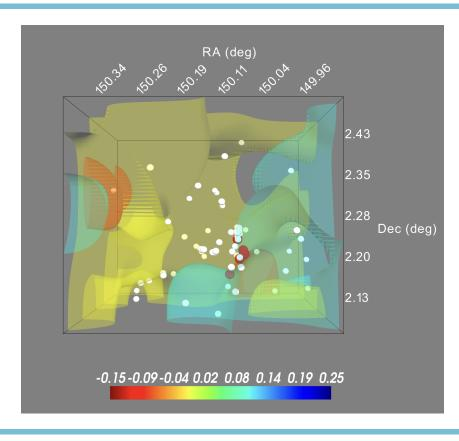


Figure 1. A preview of interactive plot (at this url) demonstrating the position of COSTCO-I members in the volume of CLAMATO. The red, yellow, cyan surfaces represent Wiener-filtered Ly $\alpha$  flux of CLAMATO smoothed with 4  $h^{-1}$  Mpc Gaussian filter,  $\delta_F^{\rm w} = -0.1, 0, 0.1$ , respectively; the white dots are positions of galaxies in the catalog by Momose et al. (2022). We emphasize the core members of COSTCO-I with red spheres, and it is clear there is no Ly $\alpha$  excess (red contours) associated with the protocluster. The static preview shows the field in the transverse plane projected over redshift range 2.27 < z < 2.33, but the online version is fully 3D with a redshift range of 2.18 < z < 2.41. In the interactive figure, users can zoom in/out and/or rotate the figure about any axis. At the bottom of the interactive figure are 4 buttons. These allow the user to reset the view back to the default orientation, a view along Right Ascension, a view along Declination, and a view along redshift.

The raw spectra were reduced, and then the unabsorbed continuum C was estimated using the meanflux regulation technique (Lee 2012). After selecting spectra with a continuum-to-noise ratio (CNR) criteria  $\langle \text{CNR} \rangle \geq 1.2$ , the final sample for 3D reconstruction comprised of 320 galaxies and quasars in total. For each spectral pixel in the rest frame  $1041\text{\AA} < \lambda < 1185\text{\AA}$ , the Ly $\alpha$  transmitted flux is defined as

$$\delta_F = \frac{f}{C\langle F \rangle(z)} - 1,\tag{4}$$

where  $\langle F \rangle(z)$  is the average transmission at a given redshift z. The processed pixel data was mapped to a comoving volume covering  $34 \, h^{-1} \, \mathrm{Mpc} \times 28 \, h^{-1} \, \mathrm{Mpc} \times 438 \, h^{-1} \, \mathrm{Mpc}$  along the R.A., Dec, and line-of-sight dimensions, respectively.

The Wiener filtering algorithm dachshund (Stark et al. 2015a) was then applied on the pixel data to create

a reconstructed map of the 3D Ly $\alpha$  absorption  $\delta_F^{\rm w}$  in the redshift range 2.05 < z < 2.55. The correlation lengths adopted for this reconstruction are  $L_{\perp} = 2.5 \, h^{-1} \, {\rm Mpc}$  and  $L_{\parallel} = 2.0 \, h^{-1} \, {\rm Mpc}$  in the transverse and line-of-sight dimensions, respectively.

Note that as part of their CLAMATO data release, Horowitz et al. (2022) also reconstructed the underlying 3D matter density field using a different constrained realization method (Horowitz et al. 2021) from COSTCO. However, this used a combination of coeval galaxy positions in addition to the Ly $\alpha$  absorption as its input, assuming an FGPA-type relationship. Since we would like to use only the Ly $\alpha$  forest transmission for this analysis, we will use the Wiener-filtered Ly $\alpha$  map instead of the matter density map. The 3D contours in Figure 1 indicate the Ly $\alpha$  absorption in the vicinity of COSTCO-I. It is clear that the region in the vicinity of COSTCO-I exhibits only average absorption ( $\delta_F^{\rm w} \sim 0$ ) instead of

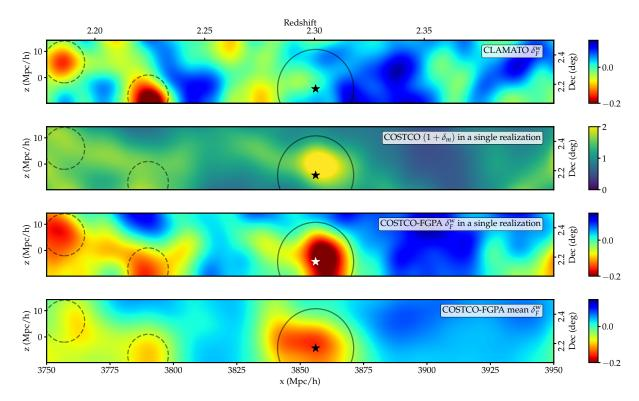


Figure 2. A series of smoothed sliceplots with thickness  $2\,h^{-1}$  Mpc (150.095 <RA< 150.125) that include the COSTCO-I galaxy protocluster, which is marked with the star. From top to bottom, the panels show the transmission of CLAMATO, the density contrast of one COSTCO constrained simulation, the transmission of the corresponding COSTCO-FGPA Ly $\alpha$  forest mock and finally the mean Ly $\alpha$  transmission averaged over all realizations. The abscissa ('x'-axis) is along the LOS dimension, while the ordinate ('z'-axis) is along increasing declination in the transverse plane. All the maps are smoothed with a  $4\,h^{-1}$  Mpc Gaussian kernel, while the circles indicate the  $r=15\,h^{-1}$  Mpc sphere over which we average in Section 3.2. In addition, we mark with dashed circles two other extended structures around the COSTCO-III (at z=2.18) and CC2.2 (at z=2.22) protoclusters, even though their barycenters are outside the plane of the slices shown here.

the strong absorption expected of a protocluster (Stark et al. 2015a; Qezlou et al. 2022)

# 3. ANALYSIS

The top panel in Figure 2 shows a narrow projected slice of the reconstructed Ly $\alpha$  transmission from CLAM-ATO, centered on the COSTCO-I coordinates, in comparison with a single realization of the matter density field that was constrained from galaxy tracers by COSTCO (second panel). In this figure, not only do we not see significant  $Lv\alpha$  absorption associated with COSTCO-I, we see significant absorption features associated with two other protoclusters reported by Ata et al. (2022): at z = 2.18 we see the extended signal from COSTCO-III, while at z = 2.22 there is a signal associated with the CC2.2 protocluster (Darvish et al. 2020, but also detected in COSTCO). In both cases, the protocluster centers actually lie outside of the map region shown in the figure, which further emphasizes the lack of signal associated with COSTCO-I.

This lack of Ly $\alpha$  absorption associated with a known galaxy protocluster appears to depart from the FGPA (Equation 2), in which matter overdensities are expected to yield strong Ly $\alpha$  absorption on scales of  $\sim$ Mpc or greater. We also checked the preliminary maps from the LATIS Survey (Newman et al. 2020), a completely independent IGM tomography survey which also targeted the COSMOS field. A visual inspection of their Figure 26 shows no excess Ly $\alpha$  absorption in the vicinity of COSTCO-I.

We now proceed to quantify this discovery by adopting as our null hypothesis that the protocluster gas associated with COSTCO-I follows the FGPA. The COSTCO constrained simulations offers a convenient way to test this null hypothesis: since its matter density field was estimated using galaxies as tracers, we can 'paint' the  $\text{Ly}\alpha$  absorption using FGPA, and incorporate the observational uncertainties of CLAMATO (e.g. sightline sampling, pixel noise, Wiener filtering).

# 3.1. COSTCO-FGPA Mock IGM Maps

We use 57 COSTCO realizations at the z=2.3 snapshot to generate the mock IGM tomography data that is matched to CLAMATO observational properties. To convert real-space matter density of COSTCO into redshift-space transmission  $F_{sim}$ , we make use of the FGPA relation (Equation 2), In our calculation, we adopt the widely-used value  $\beta=1.6$  (e.g., Kooistra et al. 2022a). Note the  $\tau$  value here is extracted from real-space; to be consistent with the observations, we shift the  $\tau$  to the redshift-space value  $\tau_{red}$ , and then compute the Ly $\alpha$  transmission in redshift space from

$$F_{sim} = \exp\left(-\tau_{red}\right) \tag{5}$$

As the proportional coefficient of the FGPA relation (Equation 2) is yet to be determined, we keep it as an unknown and solve its value by setting a mean transmission value (Becker et al. 2013)

$$\langle F_{sim} \rangle = \langle F \rangle_{z=2.30} = 0.8447 \tag{6}$$

Note that the resolution of the simulations is relatively coarse, with a grid of  $2\,h^{-1}\,\mathrm{Mpc}$ . Therefore, the resulting FGPA transmission sightlines can not be expected to accurately reproduce the small-scale statistics of the Ly $\alpha$  forest. However, the Appendix of Horowitz et al. (2021) shows that even such a coarse grid resolution should suffice to recover the structures of the cosmic web on scales of  $\sim 2\,h^{-1}\,\mathrm{Mpc}$ . We therefore do not expect the low resolution of the COSTCO suite to significantly affect our analysis.

With the simulated FGPA transmission field  $F_{sim}$  from the COSTCO suite in hand, we proceeded to generate mock skewers that reproduce the observational properties of CLAMATO as closely as possible, through the following steps:

- 1. We extract noiseless 1-dimensional  $F_{sim}$  sightlines at the [x,y,z] positions probed by the CLAMATO sightlines. This process incorporates the positions of CLAMATO sightlines in the plane of sky, as well the finite lengths of the segments along each LOS based on the redshift of the background sources. We also applied the pixel masks that were used to mask metal-line absorption in the CLAMATO spectra.
- Continuum errors were introduced using the process described by Krolewski et al. (2017). This assumed that the continuum estimation process results in 10% fluctuations in the observed transmission, i.e.

$$F_{obs} = \frac{F_{sim}}{1 + \delta_{cont}},\tag{7}$$

where  $\delta_{cont}$  is a Gaussian random deviate with mean value 0 and standard deviation 0.1.

3. Random pixel noise was added based on the signalto-noise ratio, SNR estimated for each individual CLAMATO sightline. This resulted in a final transmitted flux

$$F = F_{obs} + N_{obs}, \tag{8}$$

where Gaussian random deviate  $N_{obs}$  (with standard deviation  $\sigma = F/\text{SNR}$ ) is the noise term. Finally, we obtained  $\delta_F = F/\langle F \rangle - 1$  and computed the noise  $\sigma_F$  from the SNR value of each sightline.

For each COSTCO realization, we repeated the final noise-addition step 20 times with different noise seeds, to enhance the size of our mock sample. As a result, we have  $57 \times 20 = 1140$  sets of mock skewers with identical spatial sampling and signal-to-noise properties as CLAMATO, that were all designed to be consistent with the galaxy density field observed in the COSMOS field. We dub this the COSTCO-FGPA sample. We compile the pixel positions,  $\delta_F$  and  $\sigma_F$ , and fed them into dachshund as was done with the real CLAMATO data. In the Wiener reconstruction, we kept the correlation lengths,  $L_{\parallel} = 2\,h^{-1}\,\mathrm{Mpc}$  and  $L_{\perp} = 2.5\,h^{-1}\,\mathrm{Mpc}$ , the same as that of CLAMATO. In the Appendix, we compare the overall properties of COSTCO-FGPA with the real CLAMATO data.

The output of these mock reconstructions,  $\delta_F^{\rm w}$ , thus constitutes our null hypothesis: based on our knowledge of the COSTCO-I protocluster from the observed galaxy distribution, the COSTCO-FGPA mock data represents what we expect to see if the associated Ly $\alpha$  forest follows FGPA. Moreover, the ensemble of 1140 mock realizations represents all our uncertainties regarding the protocluster properties estimated by COSTCO (mass distribution and position) as well as those stemming from CLAMATO (sightline sampling and pixel noise).

### 3.2. Detection of Large-Scale Heating in COSTCO-I

In the third and fourth panels of Figure 2 we show the COSTCO-FGPA maps for one realization and the ensemble mean, respectively. One can immediately see the difference of  $\delta_F^{\rm w}$  between the CLAMATO and COSTCO-FGPA. The CLAMATO IGM transmission value at the position of COSTCO-I is close to the mean ( $\delta_F^{\rm w} \sim 0$ ), while from the COSTCO-FGPA realization one sees strong absorption ( $\delta_F^{\rm w} < -0.2$ ) at the same position. The presence of absorption feature in the averaged  $\delta_F$  map for COSTCO-FGPA further confirms the mock absorption feature.

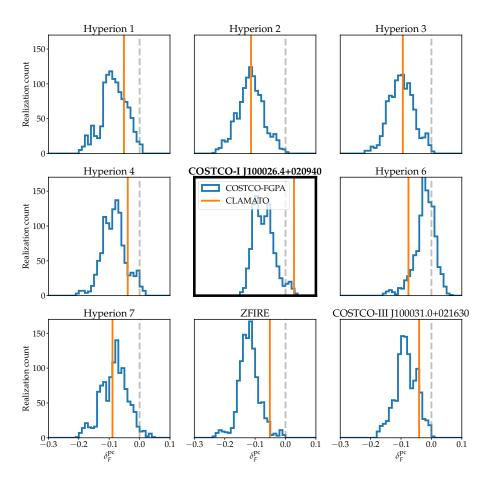


Figure 3. The distribution of  $\delta_F^{\rm pc}$  derived from the method in Section 3.2. We include all the 9 protoclusters in the overlap of CLAMATO and COSTCO volumes. The blue histogram is the distribution of  $\delta_F^{\rm pc}$  in 1140 COSTCO-FGPA mock realizations; the orange lines mark the  $\delta_F^{\rm pc}$  of corresponding protoclusters in the observed CLAMATO; the grey vertical dash lines represent  $\delta_F^{\rm pc} = 0$ . We highlight COSTCO-I with bold text (the center plot) — the mocks for this structure are clearly inconsistent with the CLAMATO measurement.

As the COSTCO-FGPA  $\delta_F^{\rm w}$  shares the same shape and coordinate system with CLAMATO  $\delta_F^{\rm w}$ , we can perform a direct, quantitative comparison between the CLAMATO and any COSTCO-FGPA realization at the position of the protocluster. First, we smooth the  $\delta_F^{\rm w}$  maps with a  $R=4\,h^{-1}$  Mpc top-hat kernel (Stark et al. 2015b), and then compute the mean  $\delta_F^{\rm w}$  value enclosed by a  $R=15\,h^{-1}$  Mpc sphere centered at the reported COSTCO-I position; we refer to this quantity as  $\delta_F^{\rm pc}$ . The radius is inspired by Ata et al. (2022), who defined a protocluster as structure that consistently formed a z=0 cluster within a  $R=15\,h^{-1}$  Mpc radius of each other in the z=0 snapshots.

We computed  $\delta_F^{\rm pc}$  centered on the protocluster for all 1140 COSTCO-FGPA realizations, and compared them with the value computed from CLAMATO. This distribution is shown in the central panel of Figure 3. The CLAMATO Ly $\alpha$  transmission associated with COSTCO-I is clearly more transparent (less ab-

sorbed) than seen in the COSTCO-FGPA mocks: we find that only 3 out of a total of 1140 COSTCO-FGPA realizations exhibit a  $\delta_F^{\rm pc}$  value greater than seen in CLAMATO. The COSTCO-FGPA mocks represent the null hypothesis that the gas in COSTCO-I is following FGPA, for which we find a probability of p =1-3/1140=0.00263 (corresponding to  $2.79\sigma$  assuming a Gaussian distribution) after incorporating all known uncertainties. This is well below the standard hypothesis testing threshold of p = 0.05, indicating a clear rejection of the null hypothesis: the protocluster gas in COSTCO-I does not follow the FGPA. Based on Equation 2, the reduced Ly $\alpha$  optical depth (i.e. increased transmission) in COSTCO-I might be due to an increase in the large-scale gas temperature, or enhanced local UV background.

COSTCO-I is not the only COSTCO-detected protocluster that falls within the CLAMATO volume. We therefore also computed  $\delta_F^{\rm pc}$  for these other protoclusters, which include well-known structures such as the ZFIRE protocluster at z=2.11 (Nanayakkara et al. 2016) and the various peaks of Hyperion at  $z\approx 2.45-2.52$  (Cucciati et al. 2018). These are shown in the noncentral panels of Figure 3, where the CLAMATO Ly $\alpha$  transmission is generally consistent with the COSTCO-CLAMATO mocks. This suggests that a transparent Ly $\alpha$  forest in protocluster gas is not an ubiquitous process at this epoch, although with we cannot rule out more subtle deviations from FGPA with the current data. Indeed, there are hints that the ZFIRE protocluster might not obey FGPA (bottom-central panel of Figure 3), but more detailed studies would be needed to confirm this.

The transparent Ly $\alpha$  forest of COSTCO-I extends across physical scales of > 4 pMpc. We have identified a compact overdensity of galaxies that forms the putative protocluster core, which would have a characteristic radius of  $r_{200} = 400 \,\text{pkpc} = 0.92 \,h^{-1} \,\text{Mpc}$  based on our estimated virial mass of  $M_V = 5.78 \times 10^{13} h^{-1} M_{\odot}$ . This is considerably smaller than the extent of the transparent gas we see in the protocluster and is therefore unlikely to be due to early formation of an intra-cluster medium (ICM). Indeed, previous studies of hot gas possibly associated with ICM formation at  $z \sim 2$  (e.g., Wang et al. 2016; Champagne et al. 2021) were on much smaller scales of  $\sim 100 \mathrm{kpc}$ . In any case, Lee et al. (2016) had tested a toy model in which the Ly $\alpha$  transmission was set to 100% transmission  $(F \equiv \exp(-\tau) = 1)$  within a  $1.5 h^{-1}$  Mpc radius of a simulated protocluster but with the gas outside following FGPA. This had a negligible effect on the averaged  $\delta_E^{\rm pc}$  computed over several Mpc, so a virialized ICM with  $r_{200} = 0.92 h^{-1} \,\mathrm{Mpc}$  cannot be responsible for the spatially extended deviation from FGPA.

We believe there are three possibilities for this largescale (> 4pMpc) protocluster heating. The first scenario is that the protocluster gas is being collisionally shockheated due to gravitational collapse of the accreting material on large scales. However, this seems disfavored by prior theoretical analysis of the large-scale Ly $\alpha$  forest signal in  $z \sim 2$  protoclusters. Miller et al. (2021) studied  $z \sim 2.4$  protoclusters within the IllustrisTNG100 hydrodynamical simulation (Weinberger et al. 2017; Pillepich et al. 2018). They found that for an uniform UV background, the effect of collisional ionization is negligible on the smoothed 3D Ly $\alpha$  forest signal associated with protoclusters. Kooistra et al. (2022b), on the other hand, performed zoom-in hydrodynamical simulations on a set of galaxy protoclusters, with various phenomenological pre-heating prescriptions of the protocluster gas. They did however perform fiducial runs where gas hydrodynamics was in effect, but no feedback or pre-heating was applied. Even in z=2 protoclusters associated with the most massive z=0 clusters  $(M(z=0)\sim 10^{15}\,h^{-1}\,M_\odot)$ , simple gravitational shock heating appears to be generally insufficient to make the  $\sim$ Mpc-scale Ly $\alpha$  absorption significantly more transparent than the canonical FGPA. These two studies, however, analyzed only a small number of simulated protoclusters:  $\sim 20$  by Miller et al. 2021 and 5 by Kooistra et al. 2022a. Therefore, while they did not find large-scale gravitational shock heating at  $z\sim 2.3$ , we cannot rule out the possibility that this is in progress in a small fraction of protoclusters. A more comprehensive study involving large numbers of simulated protoclusters would help clarify this.

The second possibility for the large-scale heating is that feedback processes from protocluster galaxies or AGN is responsible for the reduced absorption in COSTCO-I. Kooistra et al. (2022b) applied a simple phenomenological pre-heating model to protocluster gas, which imposed an entropy floor,  $K_{floor}$ , such that protocluster gas cells at z = 3 have internal gas entropy values of  $T n_e^{-2/3} > K_{\text{floor}}$ , where T is the gas temperature and and  $n_e$  is the electron density (see also Borgani & Viel 2009). Their results showed that a significant entropy floor of  $K_{\rm floor} \gtrsim 50 \ {\rm keV \ cm^{-3}}$  would be required to cause increased Ly $\alpha$  transmission to  $\delta_F \sim 0$  in  $z \sim 2$ protoclusters. Kooistra et al. (2022b) were agnostic on the possible mechanisms that could cause such preheating. Over the years, however, there has been a growing consensus that feedback from AGN is necessary to reproduce various properties related to galaxy clusters and groups (e.g., Puchwein et al. 2008; McCarthy et al. 2010). AGN feedback is included in the IllustrisTNG100 simulation analyzed by Miller et al. (2021), who showed that it does not appear to cause strong deviations from a FGPA-like relationship between the Ly $\alpha$  transmission and matter density in z = 2.44 protoclusters. However, the AGN feedback energy in the TNG model is deposited isotropically in the immediate vicinity of each SMBH. The AGN feedback in the Simba simulations (Davé et al. 2019), on the other hand, implements a collimated-jet feedback scheme for low-Eddington ratio AGN. This allows feedback energy to reach much larger scales compared with TNG (Tillman et al. 2022). AGN jet feedback also appears to be driving large-scale heating at  $z \sim 2$  in the HorizonAGN suite (Chabanier et al. 2020) with significant effects on global Ly $\alpha$  forest statistics, although they did not focus on protoclusters. At low-z, radio lobes from giant radio galaxies have been shown to extend up to  $\sim 4-5\,\mathrm{Mpc}$  (Delhaize et al. 2021; Oei et al. 2022), so similar mechanisms operating in high-redshift protoclusters could be heating up the proto-ICM over similar scales.

Finally, an enhanced local UV radiation field,  $\Gamma_{uv}$ , from AGN within the protocluster could be an alternative cause of deviations from FGPA. However, Miller et al. (2021) also considered a radiative model with a realistic quasar luminosity function in their analysis of IllustrisTNG100 protoclusters, and showed that this is unlikely to denude the Ly $\alpha$  forest absorption of protoclusters to the extent that we see in COSTCO-I. Rare hyper-luminous quasars (with absolute magnitudes of  $M_{1450} \gtrsim -27$ ) would have a more significant effect on the Ly $\alpha$  absorption (Visbal & Croft 2008; Schmidt et al. 2018) than the simulated AGN considered by Miller et al. (2021), but we see no Type-I quasars within this protocluster. On the other hand, obscured Type-II quasars emitting anisotropically away from our line-ofsight might indeed cause deviations from FGPA. Hyperluminous quasars are however rare in the Universe and we therefore deem it less unlikely cause of the Ly $\alpha$  transparency in COSTCO-I than collisional heating or jetfeedback. It would however be an exciting discovery if an obscured hyper-luminous quasar were responsible for the transparency of COSTCO-I. We will investigate this possibility in a follow-up study of the protocluster members.

# 4. CONCLUSION

In this Letter, we presented evidence that the Ly $\alpha$  forest associated with an observed galaxy protocluster at z=2.298 is considerably more transparent (i.e. less absorbed) than expected given the overdensity of the protocluster. We interpret this to be caused by elevated gas temperatures that departs from the usual FGPA relationship that governs the Ly $\alpha$  transmission as a function of underlying matter density field.

Whichever the true heating mechanism might be, the COSTCO-I galaxy protocluster appears to be the first known large-scale structure where the gas is undergoing the transition from the optically-thin photoionized temperature-density relationship of Cosmic Noon ( $z\sim 2-4$ ), into the ICM by z=0. In follow-up studies, we will study the effects of various feedback mechanisms in hydrodynamical simulations specifically in context of  $z\sim 2-3$  protoclusters, while also examining the multi-wavelength data extant in COSMOS field to search for trends in the constituent galaxies and gas associated with COSTCO-I.

### 5. ACKNOWLEDGMENTS

We thank Renyue Cen for useful discussions that helped initiate this project, and Mike Rich for useful feedback on the draft. Kavli IPMU was established by World Premier International Research Center Initiative (WPI), MEXT, Japan. C.Z.D. is supported by Forefront Physics and Mathematics Program to Drive Transformation (FoPM), a World-leading Innovative Graduate Study (WINGS) Program, the University of Tokyo. K.G.L. acknowledges support from JSPS Kakenhi grants JP18H05868 and JP19K14755. M.A. was supported by JSPS Kakenhi Grant JP21K13911. The data presented herein were obtained at the W.M. Keck Observatory, which is operated as a scientific partnership among the California Institute of Technology, the University of California and the National Aeronautics & Space Administration (NASA). The Observatory was made possible by the generous financial support of the W.M. Keck Foundation. We also wish to recognize and acknowledge the very significant cultural role and reverence that the summit of Maunakea has always had within the indigenous Hawai'ian community. We are most fortunate to have the opportunity to conduct observations from this mountain.

#### APPENDIX

In this Appendix, we compare the global properties of the COSTCO-FGPA mock maps with the CLAMATO observational data. In Figure 4, we present the probability distribution function (PDF) of CLAMATO and COSTCO-FGPA transmission field. We find that the CLAMATO and COSTCO-FGPA transmission distributions are in good agreement in the low transmission region, while the high transmission region is not well-reproduced in the mock transmission map. We attributed this to the tracers used in COSTCO, which are galaxies with known spectroscopic redshifts. According to the galaxy formation and evolution theory, galaxies are formed in the dark matter halos which are located in the density peaks. This means that reconstructions at their most reliable in high density (low Ly $\alpha$  forest transmission) regions; on contrary, the structures in the low density regions are mostly introduced by noises of mock data.

As proposed by Kooistra et al. (2022a), the Ly $\alpha$  transmission-density relation can be a diagnostic of galaxy feedback. Figure 5 depicts this relation for the whole CLAMATO volume and the COSTCO-I region. The left column shows the

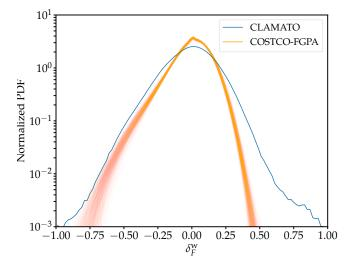


Figure 4. The distribution of  $\delta_F^{\rm w}$  values from Wiener-filtered Ly $\alpha$  absorption maps in the CLAMATO field. The orange histograms are the distribution of different realizations from the COSTCO-FGPA reconstructions, while the blue histogram is for the actual CLAMATO data. The distributions agree reasonably well in the low-transmission regime ( $\delta_F^{\rm w} \lesssim 0$ ) which traces overdensities.

relationship from one COSTCO-FGPA realization without noise, finite sightline sampling, or Wiener-filter. We find that the FGPA relation is tightly preserved after applying redshift distortions (i.e. peculiar velocities) in both the full volume and near COSTCO-I; After picking sightline sampling, adding noise, and Wiener-Filtering, the majority of the whole volume still follows the FGPA relation, while the pixels around COSTCO-I show a slightly different trend. We regard it as a consequence of information loss during the generation of mock skewers. The transmission and density in the full CLAMATO volume do show a correlation, but it is not consistent with FGPA relation of  $\beta = 1.6$ . This is likely due to additional uncertainties in the matter density construction  $(\delta_M)$  that is not reproduced in the COSTCO-FGPA relationship. Around COSTCO-I, we do not find a notable trend between the transmission and density – the  $\delta_F$  values remain almost constant. This is reminiscent of the flat transmission-density relations that have high levels of preheating as studied by Kooistra et al. (2022b). However, more quantitative studies involving the transmission-density relationship would require large observational samples and more careful modelling of systematics.

#### REFERENCES

Ata, M., Kitaura, F.-S., Lee, K.-G., et al. 2021, MNRAS, 500, 3194, doi: 10.1093/mnras/staa3318 Ata, M., Lee, K.-G., Vecchia, C. D., et al. 2022, Nature Astronomy, doi: 10.1038/s41550-022-01693-0 Becker, G. D., Hewett, P. C., Worseck, G., & Prochaska, J. X. 2013, MNRAS, 430, 2067, doi: 10.1093/mnras/stt031 Borgani, S., & Viel, M. 2009, MNRAS, 392, L26, doi: 10.1111/j.1745-3933.2008.00577.x Cai, Z., Fan, X., Peirani, S., et al. 2016, ApJ, 833, 135, doi: 10.3847/1538-4357/833/2/135 Cen, R., & Ostriker, J. P. 2006, ApJ, 650, 560, doi: 10.1086/506505 Chabanier, S., Bournaud, F., Dubois, Y., et al. 2020, MNRAS, 495, 1825, doi: 10.1093/mnras/staa1242 Champagne, J. B., Casey, C. M., Zavala, J. A., et al. 2021, ApJ, 913, 110, doi: 10.3847/1538-4357/abf4e6

Chiang, Y.-K., Overzier, R., & Gebhardt, K. 2013, ApJ, 779, 127, doi: 10.1088/0004-637X/779/2/127 Chiang, Y.-K., Overzier, R. A., Gebhardt, K., & Henriques, B. 2017, ApJL, 844, L23, doi: 10.3847/2041-8213/aa7e7b Cucciati, O., Lemaux, B. C., Zamorani, G., et al. 2018, A&A, 619, A49, doi: 10.1051/0004-6361/201833655 Darvish, B., Scoville, N. Z., Martin, C., et al. 2020, ApJ, 892, 8, doi: 10.3847/1538-4357/ab75c3 Davé, R., Anglés-Alcázar, D., Narayanan, D., et al. 2019, MNRAS, 486, 2827, doi: 10.1093/mnras/stz937 de Graaff, A., Cai, Y.-C., Heymans, C., & Peacock, J. A. 2019, A&A, 624, A48, doi: 10.1051/0004-6361/201935159 Delhaize, J., Heywood, I., Prescott, M., et al. 2021, MNRAS, 501, 3833, doi: 10.1093/mnras/staa3837 Girardi, M., Giuricin, G., Mardirossian, F., Mezzetti, M., & Boschin, W. 1998, ApJ, 505, 74, doi: 10.1086/306157

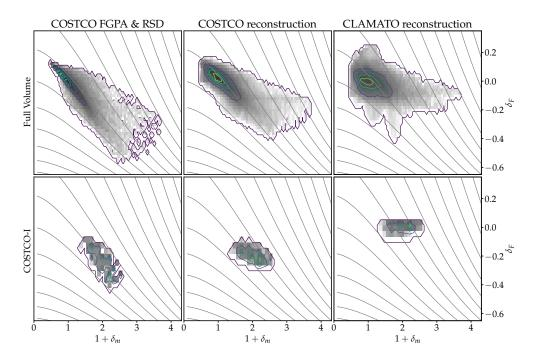


Figure 5. Top row: the transmission-density relation of the whole CLAMATO volume. Bottom row: the transmission-density relation of  $4.5\,h^{-1}\,\mathrm{Mpc}$  sphere centered at COSTCO-I. Left-most column shows the relations of underlying matter density versus  $\delta_F$  after applying FGPA & redshift-space distortions to the COSTCO matter density field; Middle column: the same after applying sightling sampling and Wiener reconstruction; Right column: the Wiener-reconstructed Ly $\alpha$  flux as seen in the real CLAMATO data. The grey lines indicates the FGPA relation  $\tau \propto (1+\delta)^{1.6}$ . All the data are spatially smoothed with a  $4\,h^{-1}\,\mathrm{Mpc}$  Gaussian kernel.

Hiss, H., Walther, M., Hennawi, J. F., et al. 2018, ApJ, 865, 42, doi: 10.3847/1538-4357/aada86
Horowitz, B., Zhang, B., Lee, K.-G., & Kooistra, R. 2021, ApJ, 906, 110, doi: 10.3847/1538-4357/abca35
Horowitz, B., Lee, K.-G., Ata, M., et al. 2022, ApJS, 263, 27, doi: 10.3847/1538-4365/ac982d
Hui, L., & Gnedin, N. Y. 1997, MNRAS, 292, 27
Hui, L., & Haiman, Z. 2003, ApJ, 596, 9, doi: 10.1086/377229
Kitaura, F.-S., Ata, M., Rodríguez-Torres, S. A., et al. 2021, MNRAS, 502, 3456, doi: 10.1093/mnras/staa3774
Kooistra, R., Inoue, S., Lee, K.-G., Cen, R., & Yoshida, N.

2022a, ApJ, 927, 53, doi: 10.3847/1538-4357/ac4cb1 Kooistra, R., Lee, K.-G., & Horowitz, B. 2022b, arXiv e-prints, arXiv:2201.10169. https://arxiv.org/abs/2201.10169

Kriek, M., Shapley, A. E., Reddy, N. A., et al. 2015, ApJS, 218, 15, doi: 10.1088/0067-0049/218/2/15

Krolewski, A., Lee, K.-G., Lukić, Z., & White, M. 2017, ApJ, 837, 31, doi: 10.3847/1538-4357/837/1/31

Le Fèvre, O., Tasca, L. A. M., Cassata, P., et al. 2015,
A&A, 576, A79, doi: 10.1051/0004-6361/201423829
Lee, K.-G. 2012, ApJ, 753, 136,

doi: 10.1088/0004-637X/753/2/136

Lee, K.-G., Hennawi, J. F., Stark, C., et al. 2014, ApJL, 795, L12, doi: 10.1088/2041-8205/795/1/L12

Lee, K.-G., Hennawi, J. F., Spergel, D. N., et al. 2015, ApJ, 799, 196, doi: 10.1088/0004-637X/799/2/196

Lee, K.-G., Hennawi, J. F., White, M., et al. 2016, ApJ, 817, 160, doi: 10.3847/0004-637X/817/2/160

Lee, K.-G., Krolewski, A., White, M., et al. 2018, ApJS, 237, 31, doi: 10.3847/1538-4365/aace58

Lilly, S. J., Le Fèvre, O., Renzini, A., et al. 2007, ApJS, 172, 70, doi: 10.1086/516589

McCarthy, I. G., Schaye, J., Ponman, T. J., et al. 2010,
MNRAS, 406, 822, doi: 10.1111/j.1365-2966.2010.16750.x
Miller, J. S. A., Bolton, J. S., & Hatch, N. A. 2021,

MNRAS, 506, 6001, doi: 10.1093/mnras/stab2083

Momose, R., Lee, K.-G., Horowitz, B., Ata, M., & Kartaltepe, J. S. 2022, arXiv e-prints, arXiv:2212.05984. https://arxiv.org/abs/2212.05984

Nanayakkara, T., Glazebrook, K., Kacprzak, G. G., et al. 2016, ApJ, 828, 21, doi: 10.3847/0004-637X/828/1/21

Newman, A. B., Rudie, G. C., Blanc, G. A., et al. 2020, ApJ, 891, 147, doi: 10.3847/1538-4357/ab75ee

2022, Nature, 606, 475, doi: 10.1038/s41586-022-04681-6
Oei, M. S. S. L., van Weeren, R. J., Hardcastle, M. J., et al. 2022, A&A, 660, A2, doi: 10.1051/0004-6361/202142778

- Overzier, R. A. 2016, A&A Rv, 24, 14, doi: 10.1007/s00159-016-0100-3
- Peirani, S., Weinberg, D. H., Colombi, S., et al. 2014, ApJ, 784, 11, doi: 10.1088/0004-637X/784/1/11
- Pillepich, A., Springel, V., Nelson, D., et al. 2018, MNRAS, 473, 4077, doi: 10.1093/mnras/stx2656
- Puchwein, E., Sijacki, D., & Springel, V. 2008, ApJL, 687, L53, doi: 10.1086/593352
- Qezlou, M., Newman, A. B., Rudie, G. C., & Bird, S. 2022, ApJ, 930, 109, doi: 10.3847/1538-4357/ac6259
- Ravoux, C., Armengaud, E., Walther, M., et al. 2020, JCAP, 2020, 010, doi: 10.1088/1475-7516/2020/07/010
- Rorai, A., Carswell, R. F., Haehnelt, M. G., et al. 2018, MNRAS, 474, 2871, doi: 10.1093/mnras/stx2862
- Schmidt, T. M., Hennawi, J. F., Lee, K.-G., et al. 2018, ArXiv e-prints. https://arxiv.org/abs/1810.05156
- Shull, J. M., Smith, B. D., & Danforth, C. W. 2012, ApJ, 759, 23, doi: 10.1088/0004-637X/759/1/23

- Sorini, D., Oñorbe, J., Lukić, Z., & Hennawi, J. F. 2016, ApJ, 827, 97, doi: 10.3847/0004-637X/827/2/97
- Stark, C. W., Font-Ribera, A., White, M., & Lee, K.-G. 2015a, MNRAS, 453, 4311, doi: 10.1093/mnras/stv1868
- Stark, C. W., White, M., Lee, K.-G., & Hennawi, J. F. 2015b, MNRAS, 453, 311, doi: 10.1093/mnras/stv1620
- $\label{eq:continuous} Tillman, M. T., Burkhart, B., Tonnesen, S., et al. 2022, arXiv e-prints, arXiv:2210.02467.$ 
  - https://arxiv.org/abs/2210.02467
- Trac, H., Cen, R., & Loeb, A. 2008, ApJL, 689, L81, doi: 10.1086/595678
- Visbal, E., & Croft, R. A. C. 2008, ApJ, 674, 660, doi: 10.1086/523843
- Wang, T., Elbaz, D., Daddi, E., et al. 2016, ApJ, 828, 56, doi: 10.3847/0004-637X/828/1/56
- Weinberger, R., Springel, V., Hernquist, L., et al. 2017, MNRAS, 465, 3291, doi: 10.1093/mnras/stw2944